

Effect of microbial biopolymers on the sedimentation behavior of kaolinite

Yeong-Man Kwon^{1,2a}, Seok-Jun Kang^{2b}, Gye-Chun Cho^{2c} and Ilhan Chang^{*3}

¹Department of Civil and Environmental Engineering, Northwestern University, Evanston, IL, 60208, USA

²Department of Civil and Environmental Engineering, KAIST, Daejeon 34141, Korea

³Department of Civil Systems Engineering, Ajou University, Su-won 16499, Korea

(Received December 24, 2022, Revised March 12, 2023, Accepted March 21, 2023)

Abstract. Clay sedimentation has been widely analyzed for its application in a variety of geotechnical constructions such as mine tailing, artificial islands, dredging, and reclamation. Chemical flocculants such as aluminum sulfate ($\text{Al}_2(\text{SO}_4)_3$), ferric chloride (FeCl_3), and ferric sulfate ($\text{Fe}(\text{SO}_4)_3$), have been adopted to accelerate the settling behaviors of clays. As an alternative clay flocculant with natural origin, this study investigated the settling of xanthan gum-treated kaolinite suspension in deionized water. The sedimentation of kaolinite in solutions of xanthan gum biopolymer (0%, 0.1%, 0.5%, 1.0%, and 2.0% in a clay mass) was measured until the sediment height was stabilized. Kaolinite was aggregated by xanthan gum via a direct electrical interaction between the negatively charged xanthan gum molecules and positively charged edge surface and via hydrogen bonding with kaolinite particles. The results revealed that the xanthan gum initially bound kaolinite aggregates, thereby forming larger floc sizes. Owing to their greater floc size, the aggregated kaolinite flocs induced by xanthan gum settled faster than the untreated kaolinite. Additionally, X-ray computed tomography images collected at various depths from the bottom demonstrated that the xanthan gum-induced aggregation resulted in denser sediment deposition. The findings of this study could inspire further efforts to accelerate the settling of kaolinite clays by adding xanthan gum.

Keywords: coagulation; flocculation; kaolinite; sedimentation; xanthan gum

1. Introduction

Gravity and electrical forces cause flocculation and subsequent sedimentation of clay particles in solution (Kynch 1952). A better understanding of the soil settling behavior can aid in several academic applications, such as the identification of sediment accumulation (Watabe and Saitoh 2015), land reclamation (Lee *et al.* 1987), mineral waste disposal (Zbik *et al.* 2008), river-floodplain morphodynamics (Lamb *et al.* 2020), colloidal chemistry (Lagaly and Ziesmer 2003), and wastewater treatment (Shaikh *et al.* 2017).

Clay particle contact processes and settling behavior have been determined using various empirical and theoretical techniques (Kynch 1952, Imai 1980, Sridharan and Prakash 1999, Wang and Siu 2006). Particle size, sediment content, organic and chemical environments, and various other variables affect the settling behavior of clay particles in suspension (Berlamont *et al.* 1993). Generally, sediments settle more quickly when the particle size, sediment container size, specific weight, and net particle attraction force are larger, while increasing sediment concentration and fluid viscosity decreases the soil settling time (Imai 1980, Toorman 1996, Chamley 2013).

Considering their surface charge properties, the Van der Waals and other net interparticle forces regulate clay interactions and sedimentation behavior (Verwey 1947, van Oss *et al.* 1990, Missana and Adell 2000). Moreover, surface charge characteristics are affected by pore chemical fluid parameters (e.g., pH and salinity), which affect the net forces between clay particles (Kotylar *et al.* 1996, Sridharan and Prakash 1999, Durán *et al.* 2000).

According to Imai (1980), the sedimentation behavior of kaolinite suspensions can be characterized as follows: dispersed settling, flocculated free settling, zone settling, and compression (Fig. 1(a)). For dispersed settling, the soils are separately stacked from bottom to top, which occurs when the soil particles disperse and settle independently of one another (Fig. 1(b)). A larger particle settles first, followed by smaller particles. However, in the flocculated settling stage, soil flocs settle with intense interactions with each other. Consequently, the soils consistently settle, forming a distinct boundary between the soil suspension and supernatant (Fig. 1(b)). In the compression stage, the soil mixture settles because of consolidation rather than the formation of visible flocs. This behavior progresses at a slower velocity than it does under other settling conditions.

Kaolinite ($\text{Al}_2\text{Si}_2\text{O}_5(\text{OH})_4$), a ubiquitous clay, is a crucial mineral in mine tailings (Zhu *et al.* 2012, Kinnunen *et al.* 2018), pharmaceuticals (Awad *et al.* 2017), photocatalysts (Cao *et al.* 2021), and 3D printing (Revelo and Colorado 2018). Kaolinite is a 1:1 layered silicate mineral with octahedral alumina (AlO_6) and tetrahedral silica (SiO_4) sheets linked by oxygen atoms. A kaolinite layer has no net electrical charge, and consequently, no large cations are

*Corresponding author, Associate Professor
E-mail: ilhanchang@ajou.ac.kr

^aPh.D.

^bPh.D.

^cProfessor

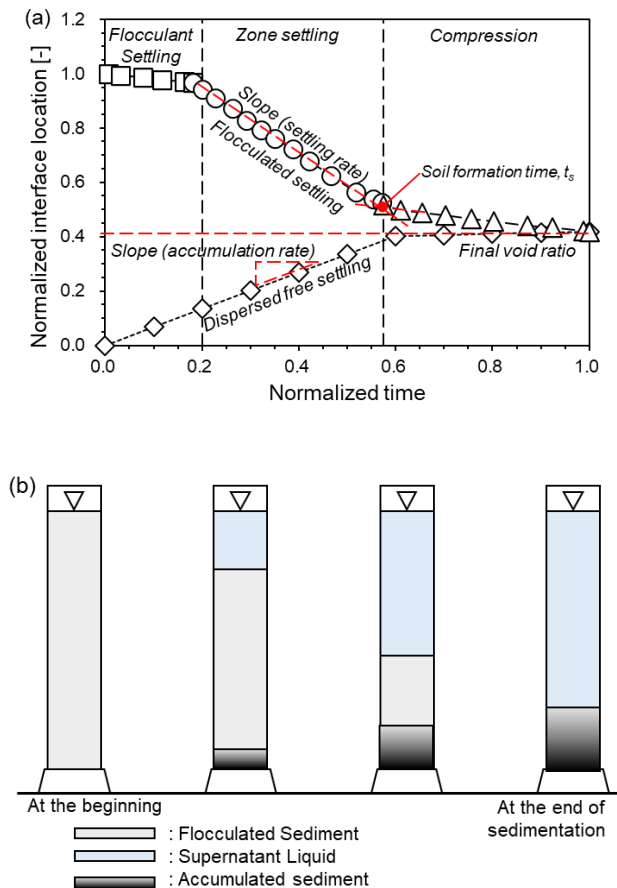


Fig. 1 Typical settling behavior of the clay suspension for (a) settling curve (Imai 1980) and (b) settling characteristics (Kaya *et al.* 2006)

present between the layers. Thus, kaolinite has a low cation exchange capacity (i.e., 6.1 meq/100 g). Furthermore, the colloidal stability, coagulation, and flocculation should be considered to effectively use kaolinites for mine tailing, wastewater treatment (Ruhling Pan *et al.* 1999), sediment transport, and reservoir sedimentation (Cheng 1997).

Especially in a high water content state, kaolinite requires the addition of a flocculant for solid-liquid separation (Du *et al.* 2010). Flocculation proceeds with particle-flocculant mixing, followed by flocculant adsorption onto the particle surface, flocculant re-formation on the particle surface, flocculation, and floc breakup induced by shear (Elimelech *et al.* 2013). Numerous scholars have analyzed the chemical properties of tailings, including the pH, ionic strength, flocculant type, charge, and adsorption capacity. For instance, polyanions can form interparticle aggregates, enlarging and accelerating the settling velocity of the clay particles. Zhou *et al.* (2008) showed that the adhesive forces of cationic polymeric flocculants and silica surfaces are dominant for determining the compressive yield stress with the aggregate size and structure. Furthermore, anionic polyacrylamide flocculants have exhibited the potential to increase settling rates and consolidation (Mpfou *et al.* 2003, McFarlane *et al.* 2005).

As shown in Fig. 2, the edge surfaces of kaolinite are known to play an essential role in anionic flocculant adsorption (Lee *et al.* 1991, Heller and Keren 2003). The protonation-deprotonation of broken bonds in the alumina layer imparts clay minerals with their pH-independent and pH-dependent charges (Mohan and Fogler 1997, Tombácz and Szekeres 2006). The basal surface of kaolinite carries a permanent pH-independent negative charge. In contrast, the edge surface has a pH-dependent charge, with a positive charge under acidic conditions and a negative charge under basic conditions (Nasser and James 2006). Thus, without flocculants, the positively charged edge of kaolinite interacts with the negatively charged face surfaces, forming heteropolar coagulation (i.e., edge-to-face (E-F) coagulation). In contrast, double-layer repulsion dominates the clay contact when the pH of the edge surface is greater than the isoelectric point. Wang and Siu (2006) found that the settling velocity decreased and the ultimate sediment density increased as the pH of the suspension increased. When moderately added, the flocculants adsorb on the edge side of kaolinite, forming edge-to-edge (E-E) flocculation. Lee *et al.* (1991) showed that 94% of polyacrylamide adsorption occur through the kaolinite edge surface. Although polyacrylamide is an effective conditioner for clay coagulation, erosion mitigation, water infiltration (Seybold 1994), and nutrient movement in soils (Kim *et al.* 2015), its residual acrylamide monomer is a neurotoxin for humans (Seybold 1994). Thus, the residual content must be maintained at levels lower than 0.05% concentration (Theodoro *et al.* 2013).

Cationic biopolymers (e.g., chitosan and ϵ -polylysine) have been demonstrated as efficient coagulating agents for clay particles (Ferhat *et al.* 2016, Kwon *et al.* 2017, Kwon *et al.* 2019). However, the application of anionic biopolymers for clay sedimentation has not yet been elucidated. Thus, the objective of this study was to investigate the effects of the xanthan gum (XG) biopolymer, a naturally produced anionic biopolymer, on the fabric development of kaolinite suspensions. XG is a natural, high-molecular-weight polysaccharide-type biopolymer. Fermentation is used to produce XG from simple sugars, and it gets its name from the bacterium *Xanthomonas campestris*, which produces XG during metabolism. XG consists of 1,4-linked β -D-glucose residues and a trisaccharide side chain (Katzbauer 1998). The glucuronic and pyruvic acid groups in the side chain give XG a highly negative charge, which enhances the hydration of XG (Latifi *et al.* 2016). The molecular weight of XG is approximately 2 tons/mol (Walter and Jacon 1994) and has many industrial applications, including being used as a common food ingredient (García-Ochoa *et al.* 2000).

As an excellent thickener, emulsifying agent, and stabilizer, XG inhibits substances from dissolving in one another. In geotechnical applications, XG has been shown to be effective in enhancing compressive strength (Chang *et al.* 2015, Dehghan *et al.* 2019, Chang *et al.* 2020), shear strength (Chang and Cho 2019, Kwon *et al.* 2021), consistency (Chang *et al.* 2021), erosion resistance (Kwon *et al.* 2020, Kwon *et al.* 2021, Seo *et al.* 2021), and hydraulic conductivity (Sujatha *et al.* 2020). Based on its

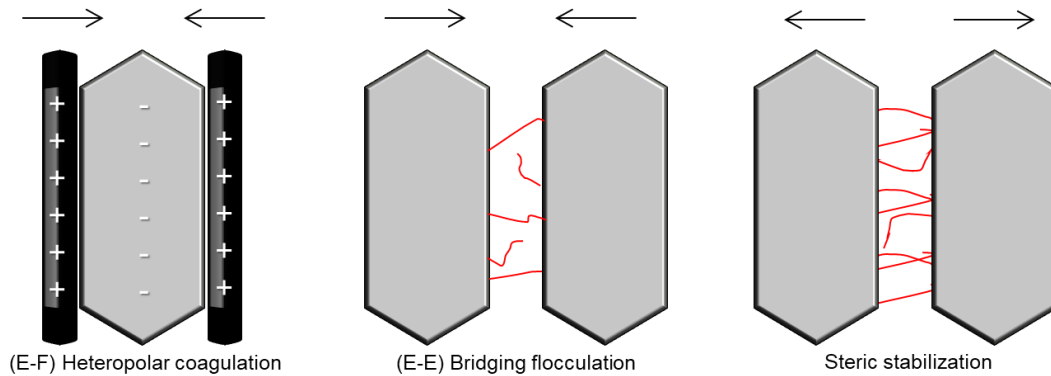


Fig. 2 Schematic depictions of kaolinite particle aggregation modes with increasing polymer concentration (Nabzar *et al.* 1984)

surface charge to bond kaolinites (Chang *et al.* 2019, Chang *et al.* 2021), we hypothesized that XG has potential for coagulating clay particles.

This study provides insights into the fabric interaction between kaolinite and XG biopolymers based on laboratory sedimentation tests. The results of sedimentation tests are analyzed based on three parameters, initial settling velocity, soil formation time, and final dry density, as reported by Kang *et al.* (2019). The X-ray computed tomography (CT) scanning analysis revealed the floc structure within the sediment that cannot be observed optically. Ultimately, the results suggest that the XG biopolymer is a promising environmentally friendly coagulant for kaolinite clay.

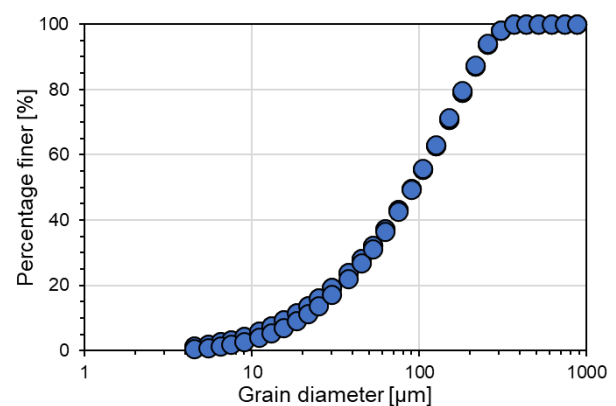


Fig. 3 Particle size distribution of kaolinite used

2. Materials and methods

2.1 Materials

Natural kaolinite from Bintang, Indonesia (CAS:1318-74-7), one of the most common minerals, was used in this study. The size distributions of kaolinite obtained using a laser scattering particle size analyzer (HELOS/KR, Sympatec GmbH, Germany) are shown in Fig. 3, and their physical properties are summarized in Table 1.

Research-grade XG purchased from Merck & Co. (CAS:11138-66-2) was utilized. The reported average molecular weight of XG is 152 kDa according to Mendes *et al.* (2012). Previous research has estimated the molecular length of XG to be approximately 1.5–3.5 μm (Whitcomb and Macosko 1978, Chang and Cho 2012), while Iijima *et al.* (2007) reported a molecular height of 1.12 nm and width of 13.91 nm.

2.2 Methods

2.2.1 Preparation of the XG-treated clay suspensions

Kaolinite sedimentation was studied by observing the settling behavior of the XG-treated kaolinite suspension (0.0%, 0.1%, 0.5%, 1.0%, and 2.0% of the XG-to-kaolinite ratio in mass) from the initial suspension stage until the sediment reached a constant volume. We used mass ratio instead of volume ratio for accuracy and reproducibility. The sample preparation process is illustrated in Fig. 4.

Table 1 Physical properties of kaolinite used in this study

OMC*	MDD*	PL**	LL**	PI**	SSA***	Gs****	USCS*****
[%]	[g/cm ³]	[%]	[%]	[%]	[cm ² /g]		
34	1.32	31	70	41	22	2.67	CH

*OMC, MDD: Optimal moisture content and maximum dry density following ASTM D698 (ASTM 2012); **PL, LL, and PI: Plastic limit, liquid limit, and plasticity index measured by ASTM D4318 (ASTM 2007); ***SSA: Specific surface area measured by methylene blue adsorption method (Santamarina *et al.* 2002); ****Gs: Specific gravity obtained following ASTM D854 (ASTM 2014); *****USCS: Unified soils classification system following ASTM D2487 (ASTM 2017)

First, the test fluid was prepared by mixing XG with deionized (DI) water using a magnetic stirrer for at least an hour to ensure uniform dissolution to mimic fluids under varying polyanion conditions (XG-to-DI water ratio in mass = 0, 0.1, 0.5, 1, and 2 g/kg). Subsequently, 50 mL of the test fluid was placed in a 25 mm diameter graduated cylinder with a maximum capacity of 100 mL. A condensed suspension of kaolinite (10 g; 3.77 mL in volume) and test fluid (50 mL) was prepared in a cylinder. The cylinder was then filled with the test fluid to a final capacity of 100 mL. Next, the XG-kaolinite suspension was gently combined by inverting the cylinder (at least 1 min of inversion), and the prepared suspensions hydrated for 24 h and then remixed (Palomino and Santamarina 2005). The cylinders were covered with a thermoplastic film (Parafilm M, USA) during inversion and experiments to prevent loss of

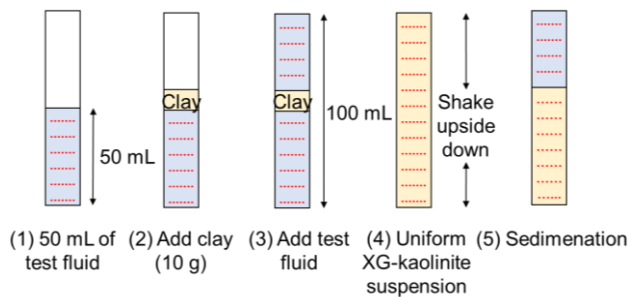


Fig. 4 Procedure for the preparation of the XG-treated kaolinite suspension

suspension and evaporation of pore-fluids. We employed a tube with a large height-to-diameter ratio (> 8) and ensured thorough mixing to minimize the wall effects, which is in line with previous studies (White 1975, White 1976, Jang *et al.* 2018).

2.2.2 Sedimentation test

The hydrated XG-kaolinite suspensions were shaken and turned upside down for at least 10 min to ensure that the components of the suspensions are homogeneously mixed and well-dispersed without introducing excessive agitation or bubbles. After the last flip, the cylinders were placed on a flat surface, and this instant was considered the beginning of sedimentation (time = 0 s). The sediment height was monitored over time using a digital camera (EOS 80D, Canon, Japan). The final sediment height was determined when the volume variation was less than 1.0 mL/d. The longest experimental duration lasted for 7 d. The temperature was controlled at 20°C, and the pH of test fluid was in the range of 6.0–6.4. According to the Angove *et al.* (1997), the zeta-potential of the face surface ranged from -3.36 to -3.59 mV while that of the edge surface ranged from 6.56 to 4.0 mV, with a pH variation of 6.0 to 6.4. After mixing with kaolinite, the acidizing effect of kaolinite occurred, and the pH dropped to 4–5, which is in line with the findings of Keller and Matlack (1990). To ensure the reliability of the experimental results, sedimentation tests were conducted in triplicate for suspensions with the same XG content.

2.2.3 Sedimentation test: Parametric analysis

The sedimentation results were divided into three representative parameters: initial settling rate, soil formation time, and final sediment density.

The initial settling rate (in mm/s), that is, the interface settling rate, is the trace of the movement of the interface formed between the dispersion and clear supernatant fluid, which is defined as the interface height, h (mm), divided by time, t (s) during the zone settling stage

$$v = \frac{h}{t}. \quad (1)$$

The initial settling rate of particles in water is affected by their diameter, density (i.e., difference in the density of

the particles and fluid), shape, roughness, and pore fluid viscosity (Loch 2001, Priya *et al.* 2015). Generally, the particles with a larger diameter, higher density, and lower pore fluid viscosity settle faster (Imai 1980).

The soil formation process can be depicted using a single sedimentation curve, flocculant settling, zone settling, and compression (Fig. 1(a)). The tangent line from the steep slope of the zone settling region intersects that from the compression region. The intersection point indicates the conclusion of the sedimentation process and the beginning of the consolidation process, signaling the abrupt settling velocity of the suspension interface. The time corresponding to the intersection point is defined as the soil formation time t_s , and the void ratio at t_s is defined as the soil formation void ratio.

The sediment density is one of the most critical factors in designing clay sedimentation for geotechnical purposes because it affects the stability and permeability of soils. The final dry density (in g/cm³) is defined as the kaolinite mass ($W_{kao} = 10$ g) divided by the final sediment volume, V_{sed} (in cm³) as Eq. (2). Here, the density of XG was not considered because of its small amount (0–2 % weight of kaolinite) and no significant effect on fluid density ($< 0.5\%$ variation in fluid density).

$$\gamma_d = \frac{W_{kao}}{V_{sed}}. \quad (2)$$

2.2.4 X-ray CT image

An X-ray CT scanner (X-eye PCT, SEC, Korea) can provide quantitative, spatially resolved information regarding the X-ray attenuation properties of the scanned region, which can be associated with the flocc and textures of the sediment.

When the sediment height stabilized, sedimentation tubes for untreated and 2%-XG-treated kaolinites were placed directly into the CT machine without any further processing. X-ray CT scanning was conducted using a source voltage of 150 kV and a current of 1 A. The maximum scan length was 120 mm, which covered the entire sediment height. All the slice images were 1024 × 1024 pixels in size. A total of 1024 thin slices covered the sediments entirely. The density and void ratio values of each slice image were determined by correlating the X-ray CT values with known-density materials through pre-calibration data.

3. Results and analysis

3.1 Settling behavior of XG-treated kaolinite suspensions

The vertical time series constructed from five experiments with XG-treated kaolinite settling in DI are plotted in Fig. 5(a). The consistency of the experimental results is corroborated by the variation observed in the triplicate experiments shown in Fig. 5(a), where the data points represent the mean values. Under pure DI water conditions without XG, kaolinite settles in a flocculated form. Considering the solid mutual interactions between the

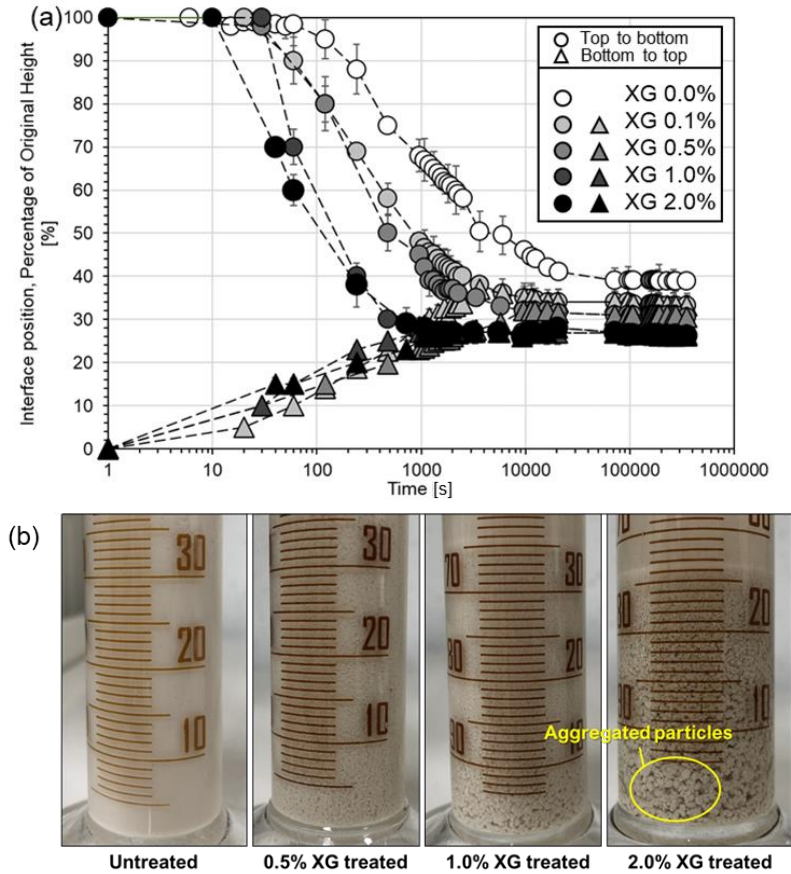


Fig. 5 Settling behavior of kaolinite with various XG contents

positively charged edges and negatively charged face surfaces (Fam and Santamarina 1997), untreated kaolinite shows uniform sedimentation of large flocs (i.e., flocculated zone settling) (Imai 1980), creating a sharp interface between the supernatant and flocculated kaolinite suspensions.

However, the XG biopolymer in DI causes a distinct change in the sedimentation behavior of kaolinite (Fig. 5(a)). The addition of XG results in a larger kaolinite floc than that in the DI water. During settling, the electrical force between the negatively charged XG molecules and positively charged edge surface of kaolinite brings the kaolinite particles together (Nugent *et al.* 2009, Chang *et al.* 2019), forming larger flocs. Furthermore, XG and kaolinite interact through exchangeable cations (Mortensen 1957, Theng 2012). Given the formation of different-sized flocs by XG-induced particle bonding, XG-treated kaolinites settle non-uniformly, that is, larger flocs settle first, followed by the gradual settling of the individual particles without XG-induced bonding. According to Stokes' law, the flocs that have been coagulated by XG settle first, followed by the smaller flocs (i.e., flocculated free settling).

Therefore, the floc sizes get more dispersed with more XG treatment in DI water. As shown in Fig. 5(b), aggregated particles are stacked at the bottom of the XG-treated sediments, whereas uniform sediments are observed for the untreated sediments. This tendency results in a mixture of dispersed and flocculated settling.

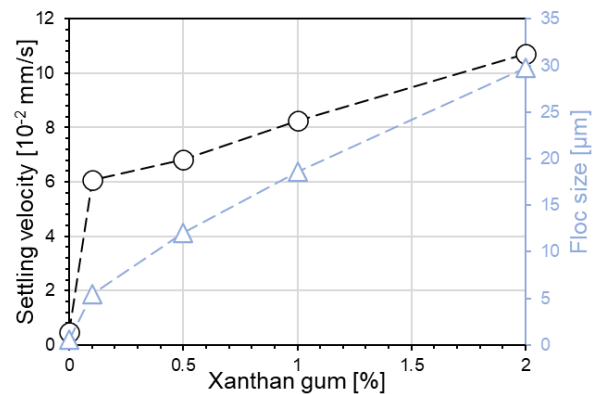


Fig. 6 Variation of initial settling rate and estimated floc size with XG content

3.2 Initial settling rate, final sediment height, and soil formation time

The initial settling rate of a suspension is an important parameter for evaluating the settling speed and stability of colloidal systems (Kang *et al.* 2019). Fig. 6 depicts the variation in the initial settling rate with XG treatment. The addition of XG to the suspension increases the settling rate of the kaolinite specimens. In detail, untreated kaolinite initially settles at a rate of 0.48×10^{-2} mm/s, whereas the initial settling rate of kaolinite increases to 10.72×10^{-2} mm/s with 2%-XG treatment. The initial settling rate

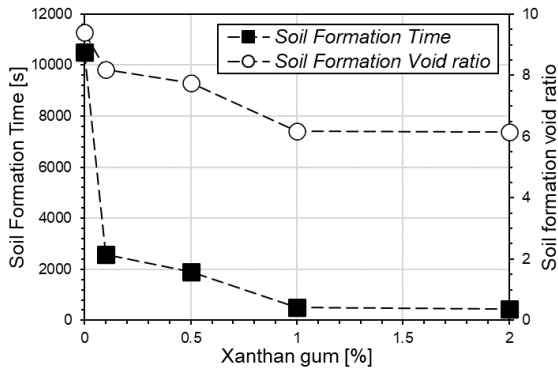


Fig. 7 Soil formation time and void ratio of kaolinite with different XG contents

increases because of the formation of the XG-induced kaolinite flocs.

The floc size during the flocculated settling stage has been estimated based on the Stokes-Einstein equation (Stokes 1851, Einstein 1905), which relates it to the size of a spherical particle as

$$r = \sqrt{\frac{9v\eta}{2g(\rho_p - \rho_f)}}, \quad (2)$$

where r (in mm/s) is the radius of flocs, v (in mm/s) is the settling velocity, η (in Pa-s) is the fluid viscosity, g is the gravimetric acceleration (9.81 m/s^2), ρ_p is the density of particle (2.67 g/cm^3), and ρ_f is the density of fluids (1 g/cm^3). Here, the value of the viscosity of XG hydrogel was taken from Khan and Yusuf (2018).

Larger flocs settle faster and contain most of the vertical settling flux of solids (Fennessy *et al.* 1997). Winterwerp (1998) also developed a model that correlates the settling velocity with the floc size and fractal dimensions. Thus, larger XG-induced flocs can increase the initial settling rate of the suspension. A small amount of XG affects the initial settling ($<0.1\%$ of the soil mass) and increases linearly with additional XG content. Thus, even a small amount of XG can result in faster settling of the kaolinite.

The soil formation time and void ratio at the time of soil formation are shown in Fig. 7. As the XG content increases, the soil formation time decreases. Compared with the case of untreated kaolinite, XG can induce a higher settling rate by forming larger flocs (Fig. 6), leading to a shorter soil formation time under the same kaolinite and pore fluid conditions. Untreated kaolinite requires 10,500 s for soil formation, whereas 2% XG-treated kaolinite requires only 442 s. The void ratio at the soil formation time also decreases with XG treatment, indicating that the XG treatment accelerates the kaolinite floc settling and densifies the kaolinite sediments in suspension.

The final sediment dry densities of the kaolinite suspensions are plotted as a function of their XG contents in Fig. 8. The final sediment dry density increases as the XG content increases. The final sediment without XG shows a dry density of 0.25 g/cm^3 , whereas XG densifies the sediment, yielding a final dry density of 0.38 g/cm^3 with 2%-XG treatment. In contrast, the 1% and 2% XG-treated kaolinites show similar soil formation times (Fig. 7) and

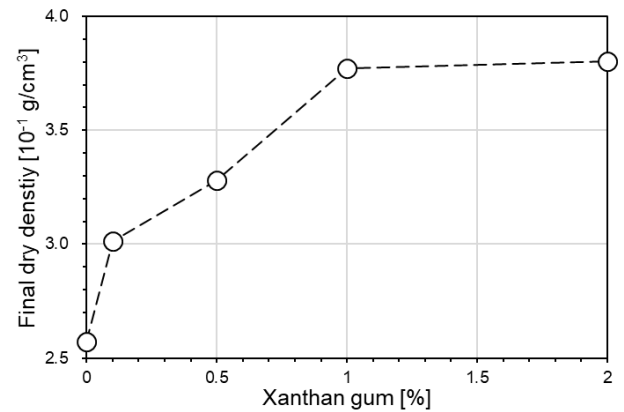


Fig. 8 Final sediment dry density of kaolinite with different XG contents

final dry densities (Fig. 8). Thus, an optimal XG content can yield a good performance and feasible material costs. This experimental condition has shown 1% of XG as an optimal XG content. Further research to optimize the XG content at a variety of conditions (e.g., mineral properties, pore-fluid composition, and solid concentration) is required.

4. Discussion

4.1 Effects of XG on the microfabric development of kaolinite

Our results show that the addition of XG polymers led to the flocculation of kaolinite particles. Given that XG molecules are in the same length range as kaolinite particles (Fig. 2), kaolinite flocculation can occur through XG bridging. Tan *et al.* (2014) analyzed the particle size of expansive clays treated with XG and showed that XG increased the particle size by flocculating the clay particles, which can be partially soluble in water forming a hydrated layer around the kaolinite particles. Specifically, the floc size increased by the electrostatic attraction between XG and kaolinite edges at $\text{pH} < 7$, and the hydrogen bonding between the carboxyl groups consisting of the XG side chain and oxygen of the clay minerals (Theng 2012). Furthermore, van der Waals attraction can contribute to the particle flocculation (O'Brien 1971).

We also noted that XG-induced kaolinite flocculation increases the initial settling rate (Fig. 6) and decreases the soil formation time (Fig. 7). With respect to the initial settling rate, even a small amount of XG ($<0.1\%$ of soil mass) is sufficient for bridging kaolinites together, thereby forming larger flocs. The formation of bridge between kaolinite particles (dominated by electrostatic attraction between XG and edge of kaolinite) links the edges of kaolinite particles forming a more compact aggregation such as face to face (Chang *et al.* 2015) and/or edge to edge (Kang *et al.* 2019), accumulating the flocs into a dense formation and resulting in a dense final sediment (Fig. 8). In summary, XG-induced particle flocculation enhances the settling efficiency of kaolinite sediments in terms of the settling rate and density of the final sediments. However,

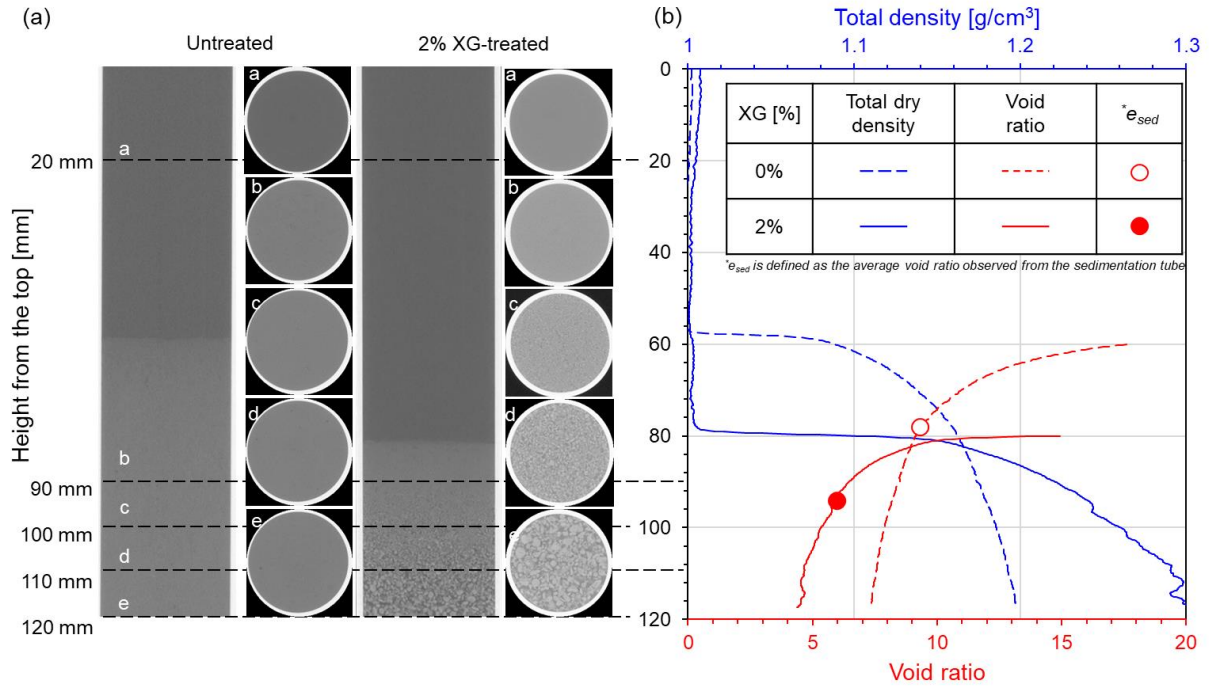


Fig. 9 X-ray CT measurements for kaolinite suspension with XG treatment for (a) vertical and horizontal slices at heights of 20, 90, 100, 110, and 120 mm from the top and (b) spatial variations of the total density and void ratio

further studies are required to consider the effects of higher viscosity by XG treatment and individual kaolinite particles remaining in the supernatant. Both parameters can hinder the settling efficiency of clay minerals. Moreover, despite previous studies indicating long-term durability of XG treatment (Lee *et al.* 2022, Kwon *et al.* 2023), biodegradation may occur due to its natural origin (Cadmus *et al.* 1982). Thus, future studies should take into account the long-term durability of XG treatment.

4.2 Density variation observed by X-ray CT imaging

The X-ray CT scanned images were captured after settling to observe the visual variations in the sediments inside the specimens and to analyze the vertical variations of the sediments in terms of total density and void ratio.

Fig. 9(a) shows the vertical and horizontal images, captured at 20, 90, 100, 110, and 120 mm from the top of the kaolinite sediments after settling was complete. The interface between the sediment and pore fluids can be distinguished in the observed images, and the pore-fluid regions of both the specimens show similar X-ray attenuation properties (i.e., mean grey value). Considering the XG-induced particle aggregation, the final sediment height decreased with XG treatment. Untreated kaolinite has a uniform horizontal surface regardless of its height from the surface. In contrast, the images of the XG-treated sediments show spatial variations, that is, larger flocs are observed near the bottom of the specimens. Thus, X-ray CT scanning confirms that XG forms dense aggregates with larger pore sizes between the aggregates.

Fig. 9(b) shows the variations in the total density and void ratio of each specimen with the scanned height (0–120

mm). In both the cases, total dry density increases with a larger height from the top. The total dry density of the untreated kaolinite is less than 1.18 g/cm³, whereas that of the XG-2% treated kaolinite is higher than that even at a height of 90 mm. Furthermore, the XG treatment increases the total density range compared to that of the untreated kaolinite. A larger deviation in dry density is induced by the formation of XG-bridged flocs.

4.3 Void ratio variation observed by X-ray CT imaging

The void ratio was calculated from the interface height (i.e., a height of 57 mm for untreated and 80 mm for XG-2% treated kaolinite), which is the height at which the total density significantly increases. The presence of a high void ratio near the kaolinite-water interface was particularly notable, with a measurement of 60 mm for untreated samples and 80 mm for XG-2% treated samples due to their proximity to water. Interestingly, the void ratio obtained through X-ray CT scanning aligns with the average void ratio calculated using the sedimentation tube method (circles in Fig 9b).

The void ratio was found to decrease from the top for both the untreated and XG-treated kaolinite sediments owing to the consolidation after settling. Even though larger voids were observed between XG-kaolinite aggregates (Fig. 5(b)), the void ratio still decreased with depth for XG-treated kaolinite, indicating that the XG-induced aggregates increased the amount of macropores (pores between the aggregates), while reducing the number of micropores (pores within individual aggregates). This suggests that XG-treatment has the potential to improve the hydraulic conductivity of soil media while forming a denser sediment.

Further studies can include analyzing the pore size distribution using techniques like mercury invasion porosimetry, and comparing the consolidation and hydraulic conductivity of XG-treated kaolinite after settling. The XG-treated sediments exhibit smaller void ratios than the untreated kaolinites. Specifically, the XG-treated kaolinite reaches a void ratio of 5 at the bottom, whereas the untreated kaolinite shows a minimum void ratio of 7 at the bottom. In summary, X-ray CT imaging efficiently reveals a higher flocculation efficiency of XG for kaolinite settling inside the sediment.

5. Conclusions

The experimental results obtained in this study elucidate the effects of XG on kaolinite sedimentation. When kaolinite is treated with XG, the particles aggregate because of the electrical charges of the XG molecules. The XG and kaolinite interact by direct bonding between the negatively charged XG side chain and positively charged edge site of kaolinite and by hydrogen bonding between the carboxyl groups consisting of the XG side chain and the oxygen in clay minerals. The bonding between kaolinite particles by XG enlarged the floc size. The larger flocs of XG-treated kaolinite increase the initial settling rate and decrease the soil formation time. The X-ray CT scanning images revealed that the heterogeneous floc sizes induced by the XG treatment result in sediment fabric differences by height from the bottom. Furthermore, the XG-induced kaolinite flocs formed dense clusters, enhancing the density and void ratio in terms of soil stabilization. These results demonstrate the efficiency of XG as an alternative flocculant for clay minerals, indicating that it has the potential to be applied for the dredging, reclamation, and construction of artificial islands. The results also clarify the effects of XG on the consolidation behaviors of the final sediments.

To extend the scope of this fundamental study, a range of experimental conditions, including the characteristics of clay minerals, chemical properties of pore-fluid, and solid fraction in suspension, must be analyzed. Additionally, further analysis is required to accurately quantify the amount of XG present in the supernatant after sedimentation.

Acknowledgments

This research was financially supported by the Ministry of Oceans and Fisheries (MOF) of the Korean Government (Project No. 20220364), and the National Research Foundation of Korea (NRF) grant funded by the Korea government (MSIT) (No. 2022R1A2C2091517).

References

Angove, M.J., Johnson, B.B. and Wells, J.D. (1997), "Adsorption of cadmium(ii) on kaolinite", *Colloids and Surfaces A: Physicochemical and Engineering Aspects*, **126**(2), 137-147. [https://doi.org/10.1016/S0927-7757\(96\)03990-8](https://doi.org/10.1016/S0927-7757(96)03990-8).

- ASTM (2007), *D4318-05: Standard test methods for liquid limit, plastic limit, and plasticity index of soils*, ASTM International, West Conshohocken.
- ASTM (2012), *D698-12e2: Standard test methods for laboratory compaction characteristics of soil using standard effort (12 400 ft-lbf/ft³ (600 kn-m/m³))*, ASTM International, West Conshohocken, PA.
- ASTM (2014), *D854-14: Standard test methods for specific gravity of soil solids by water pycnometer*, ASTM International, West Conshohocken, PA.
- ASTM (2017), *D2487-17: Standard practice for classification of soils for engineering purposes (unified soil classification system)*, ASTM International, West Conshohocken.
- Awad, M.E., López-Galindo, A., Setti, M., El-Rahmany, M.M. and Iborra, C.V. (2017), "Kaolinite in pharmaceuticals and biomedicine", *Int. J. Pharmaceutics*, **533**(1), 34-48. <https://doi.org/10.1016/j.ijpharm.2017.09.056>.
- Berlamont, J., Ockenden, M., Toorman, E. and Winterwerp, J. (1993), "The characterisation of cohesive sediment properties", *Coast. Eng.*, **21**(1), 105-128. [https://doi.org/10.1016/0378-3839\(93\)90047-C](https://doi.org/10.1016/0378-3839(93)90047-C).
- Cadmus, M.C., Jackson, L.K., Burton, K.A., Plattner, R.D. and Slodki, M.E. (1982), "Biodegradation of xanthan gum by *Bacillus* sp", *Appl. Environ. Microb.*, **44**(1), 5-11. <https://doi.org/10.1128/aem.44.1.5-11.1982>.
- Cao, Z., Wang, Q. and Cheng, H. (2021), "Recent advances in kaolinite-based material for photocatalysts", *Chinese Chem. Lett.*, **32**(9), 2617-2628. <https://doi.org/10.1016/j.ccl.2021.01.009>.
- Chamley, H. (2013), *Clay sedimentology*, Springer, Berlin, Heidelberg.
- Chang, I. and Cho, G.C. (2012), "Strengthening of Korean residual soil with β -1,3/1,6-glucan biopolymer", *Constr. Build. Mater.*, **30** 30-35. <https://doi.org/10.1016/j.conbuildmat.2011.11.030>.
- Chang, I. and Cho, G.C. (2019), "Shear strength behavior and parameters of microbial gellan gum-treated soils: From sand to clay", *Acta Geotechnica*, **14**(2), 361-375. <https://doi.org/10.1007/s11440-018-0641-x>.
- Chang, I., Im, J., Prasadhi, A.K. and Cho, G.C. (2015), "Effects of xanthan gum biopolymer on soil strengthening", *Constr. Build. Mater.*, **74**, 65-72. <https://doi.org/10.1016/j.conbuildmat.2014.10.026>.
- Chang, I., Kwon, Y.M. and Cho, G.C. (2021), "Effect of pore-fluid chemistry on the undrained shear strength of xanthan gum biopolymer-treated clays", *J. Geotech. Geoenviron. Eng.*, **147**(11), 06021013. [https://doi.org/10.1061/\(ASCE\)GT.1943-5606.0002652](https://doi.org/10.1061/(ASCE)GT.1943-5606.0002652).
- Chang, I., Kwon, Y.M., Im, J. and Cho, G.C. (2019), "Soil consistency and interparticle characteristics of xanthan gum biopolymer-containing soils with pore-fluid variation", *Can. Geotech. J.*, **56**(8), 1206-1213. <https://doi.org/10.1139/cgj-2018-0254>.
- Chang, I., Lee, M., Tran, A.T.P., Lee, S., Kwon, Y.M., Im, J. and Cho, G.C. (2020), "Review on biopolymer-based soil treatment (bpst) technology in geotechnical engineering practices", *Transport. Geotech.*, **24**, 100385. <https://doi.org/10.1016/j.trgeo.2020.100385>.
- Chang, I., Prasadhi, A.K., Im, J. and Cho, G.C. (2015), "Soil strengthening using thermo-gelation biopolymers", *Constr. Build. Mater.*, **77**, 430-438. <http://dx.doi.org/10.1016/j.conbuildmat.2014.12.116>.
- Cheng, N.S. (1997), "Effect of concentration on settling velocity of sediment particles", *J. Hydraulic Eng.*, **123**(8), 728-731. [https://doi.org/10.1061/\(ASCE\)0733-9429\(1997\)123:8\(728\)](https://doi.org/10.1061/(ASCE)0733-9429(1997)123:8(728)).
- Dehghan, H., Tabarsa, A., Latifi, N. and Bagheri, Y. (2019), "Use of xanthan and guar gums in soil strengthening", *Clean Technol. Environ. Policy*, **21**(1), 155-165.

- <https://doi.org/10.1007/s10098-018-1625-0>.
- Du, J., Morris, G., Pushkarova, R.A. and St. C. Smart, R. (2010), "Effect of surface structure of kaolinite on aggregation, settling rate, and bed density", *Langmuir*, **26**(16), 13227-13235. <https://doi.org/10.1021/la100088n>.
- Durán, J.D.G., Ramos-Tejada, M.M., Arroyo, F.J. and González-Caballero, F. (2000), "Rheological and electrokinetic properties of sodium montmorillonite suspensions: I. Rheological properties and interparticle energy of interaction", *J. Colloid Interface Sci.*, **229**(1), 107-117. <https://doi.org/10.1006/jcis.2000.6956>.
- Einstein, A. (1905), "On the movement of small particles suspended in a stationary liquid demanded by the molecular-kinetic theory of heat (english translation, 1956)", *Investigations on the theory of the Brownian movement*.
- Elimelech, M., Gregory, J. and Jia, X. (2013), *Particle deposition and aggregation: Measurement, modelling and simulation*, Butterworth-Heinemann.
- Fam, M. and Santamarina, J.C. (1997), "A study of consolidation using mechanical and electromagnetic waves", *Geotechnique*, **47**(2), 203-219.
- Fennessy, M., Dyer, K., Huntley, D. and Bale, A. (1997), "Estimation of settling flux spectra in estuaries using inssev", *Cohesive Sediments*, 87-104.
- Ferhat, M., Kadouche, S., Drouiche, N., Messaoudi, K., Messaoudi, B. and Lounici, H. (2016), "Competitive adsorption of toxic metals on bentonite and use of chitosan as flocculent coagulant to speed up the settling of generated clay suspensions", *Chemosphere*, **165**, 87-93. <https://doi.org/10.1016/j.chemosphere.2016.08.125>.
- García-Ochoa, F., Santos, V., Casas, J. and Gomez, E. (2000), "Xanthan gum: Production, recovery, and properties", *Biotechnol. Adv.*, **18**(7), 549-579.
- Heller, H. and Keren, R. (2003), "Anionic polyacrylamide polymer adsorption by pyrophyllite and montmorillonite", *Clays Clay Miner.*, **51**(3), 334-339. <https://doi.org/10.1346/CCMN.2003.0510310>.
- Iijima, M., Shinozaki, M., Hatakeyama, T., Takahashi, M. and Hatakeyama, H. (2007), "Afm studies on gelation mechanism of xanthan gum hydrogels", *Carbohydrate Polymers*, **68**(4), 701-707. <https://doi.org/10.1016/j.carbpol.2006.08.004>.
- Imai, G. (1980), "Settling behavior of clay suspension", *Soils Found.*, **20**(2), 61-77. https://doi.org/10.3208/sandf1972.20.2_61.
- Jang, J., Cao, S.C., Stern, L.A., Jung, J. and Waite, W.F. (2018), "Impact of pore fluid chemistry on fine-grained sediment fabric and compressibility", *J. Geophys. Res.: Solid Earth*, **123**(7), 5495-5514. <https://doi.org/10.1029/2018JB015872>.
- Kang, X., Xia, Z., Chen, R., Sun, H. and Yang, W. (2019), "Effects of inorganic ions, organic polymers, and fly ashes on the sedimentation characteristics of kaolinite suspensions", *Appl. Clay Sci.*, **181**, 105220. <https://doi.org/10.1016/j.clay.2019.105220>.
- Katzbauer, B. (1998), "Properties and applications of xanthan gum", *Polymer Degradation Stability*, **59**(1), 81-84. [https://doi.org/10.1016/S0141-3910\(97\)00180-8](https://doi.org/10.1016/S0141-3910(97)00180-8).
- Kaya, A., Ören, A.H. and Yükselen, Y. (2006), "Settling of kaolinite in different aqueous environment", *Mar. Georesour. Geotechnol.*, **24**(3), 203-218. <https://doi.org/10.1080/10641190600788429>.
- Keller, W.D. and Matlack, K. (1990), "The ph of clay suspensions in the field and laboratory, and methods of measurement of their ph", *Appl. Clay Sci.*, **5**(2), 123-133. [https://doi.org/10.1016/0169-1317\(90\)90018-K](https://doi.org/10.1016/0169-1317(90)90018-K).
- Khan, S.H.A. and Yusuf, M. (2018), "Studies on rheological behavior of xanthan gum solutions in presence of additives", *Pet Petrochem. Eng. J.*, **2**(5), 000165.
- Kim, M., Song, I., Kim, M., Kim, S., Kim, Y., Choi, Y. and Seo, M. (2015), "Effect of polyacrylamide application on water and nutrient movements in soils", *J. Agricultural Chem. Environ.*, **4**(3), 76. <https://doi.org/10.4236/jacen.2015.43008>.
- Kinnunen, P., Ismailov, A., Solismaa, S., Sreenivasan, H., Räisänen, M.L., Levänen, E. and Illikainen, M. (2018), "Recycling mine tailings in chemically bonded ceramics – a review", *J. Clean. Prod.*, **174**, 634-649. <https://doi.org/10.1016/j.jclepro.2017.10.280>.
- Kotylar, L.S., Sparks, B.D. and Schutte, R. (1996), "Effect of salt on the flocculation behavior of nano particles in oil sands fine tailings", *Clays Clay Min.*, **44**(1), 121-131. <https://doi.org/10.1346/CCMN.1996.0440111>.
- Kwon, Y.-M., Chang, I. and Cho, G.-C. (2023), "Consolidation and swelling behavior of kaolinite clay containing xanthan gum biopolymer", *Acta Geotechnica*, <https://doi.org/10.1007/s11440-023-01794-8>.
- Kwon, Y.-M., Chang, I., Lee, M. and Cho, G.C. (2019), "Geotechnical engineering behaviors of biopolymer-treated soft marine soil", *Geomech. Eng.*, **17**(5), 453-464. <https://doi.org/10.12989/gae.2019.17.5.453>.
- Kwon, Y.M., Cho, G.C., Chung, M.K. and Chang, I. (2021), "Surface erosion behavior of biopolymer-treated river sand", *Geomech. Eng.*, **25**(1), 49-58. <https://doi.org/10.12989/gae.2021.25.1.049>.
- Kwon, Y.M., Cho, G.C., Chung, M.K. and Chang, I. (2021), "Surface erosion behavior of biopolymer-treated river sand", *Geomech. Eng.*, **25**(1), 49-58. <https://doi.org/10.12989/gae.2021.25.1.049>.
- Kwon, Y.M., Ham, S.M., Kwon, T.H., Cho, G.C. and Chang, I. (2020), "Surface-erosion behaviour of biopolymer-treated soils assessed by efa", *Géotechnique Lett.*, **10**(2), 1-7. <https://doi.org/10.1680/jgele.19.00106>.
- Kwon, Y.M., Im, J., Chang, I. and Cho, G.C. (2017), "E-polylysine biopolymer for coagulation of clay suspensions", *Geomech. Eng.*, **12**(5), 753-770. <http://doi.org/10.12989/gae.2017.12.5.753>.
- Kynch, G.J. (1952), "A theory of sedimentation", *Transactions of the Faraday Soc.*, **48**, 166-176. <https://doi.org/10.1039/TF9524800166>.
- Lagaly, G. and Ziesmer, S. (2003), "Colloid chemistry of clay minerals: The coagulation of montmorillonite dispersions", *Adv. Colloid Interface Sci.*, **100-102**, 105-128. [https://doi.org/10.1016/S0001-8686\(02\)00064-7](https://doi.org/10.1016/S0001-8686(02)00064-7).
- Lamb, M.P., de Leeuw, J., Fischer, W.W., Moodie, A.J., Venditti, J.G., Nittrouer, J.A., Hought, D. and Parker, G. (2020), "Mud in rivers transported as flocculated and suspended bed material", *Nature Geosci.*, **13**(8), 566-570. <https://doi.org/10.1038/s41561-020-0602-5>.
- Latifi, N., Horpibulsuk, S., Meehan, C.L., Majid, M.Z.A. and Rashid, A.S.A. (2016), "Xanthan gum biopolymer: An eco-friendly additive for stabilization of tropical organic peat", *Environ. Earth Sci.*, **75**(9), 825.
- Lee, L.T., Rahbari, R., Lecourtier, J. and Chauveteau, G. (1991), "Adsorption of polyacrylamides on the different faces of kaolinites", *J. Colloid Interface Sci.*, **147**(2), 351-357. [https://doi.org/10.1016/0021-9797\(91\)90167-7](https://doi.org/10.1016/0021-9797(91)90167-7).
- Lee, M., Kwon, Y.M., Park, D.Y., Chang, I. and Cho, G.C. (2022), "Durability and strength degradation of xanthan gum based biopolymer treated soil subjected to severe weathering cycles", *Scientific Reports*, **12**(1), 19453. <https://doi.org/10.1038/s41598-022-23823-4>.
- Lee, S.L., Karunaratne, G.P., Yong, K.Y. and Ganeshan, V. (1987), "Layered clay-sand scheme of land reclamation", *J. Geotech. Eng.*, **113**(9), 984-995. [https://doi.org/10.1061/\(ASCE\)0733-9410\(1987\)113:9\(984\)](https://doi.org/10.1061/(ASCE)0733-9410(1987)113:9(984)).
- Loch, R.J. (2001), "Settling velocity – a new approach to assessing

- soil and sediment properties”, *Comput. Electron. Agric.*, **31**(3), 305-316. [https://doi.org/10.1016/S0168-1699\(00\)00189-7](https://doi.org/10.1016/S0168-1699(00)00189-7).
- McFarlane, A.J., Bremmell, K.E. and Addai-Mensah, J. (2005), “Optimising the dewatering behaviour of clay tailings through interfacial chemistry, orthokinetic flocculation and controlled shear”, *Powder Technol.*, **160**(1), 27-34. <https://doi.org/10.1016/j.powtec.2005.04.046>.
- Mendes, A.C., Baran, E.T., Pereira, R.C., Azevedo, H.S. and Reis, R.L. (2012), “Encapsulation and survival of a chondrocyte cell line within xanthan gum derivative”, *Macromol. Biosci.*, **12**(3), 350-359. <https://doi.org/10.1002/mabi.201100304>.
- Missana, T. and Adell, A. (2000), “On the applicability of dlvo theory to the prediction of clay colloids stability”, *J. Colloid Interface Sci.*, **230**(1), 150-156. <https://doi.org/10.1006/jcis.2000.7003>.
- Mohan, K.K. and Fogler, H.S. (1997), “Effect of ph and layer charge on formation damage in porous media containing swelling clays”, *Langmuir*, **13**(10), 2863-2872. <https://doi.org/10.1021/la960868w>.
- Mortensen, J.L. (1957), “Adsorption of hydrolyzed polyacrylonitrile on kaolinite: I. Effect of exchange cation and anion”, *Soil Sci. Soc. Am. J.*, **21**(4), 385-388. <https://doi.org/10.2136/sssaj1957.03615995002100040008x>.
- Mpofu, P., Addai-Mensah, J. and Ralston, J. (2003), “Influence of hydrolyzable metal ions on the interfacial chemistry, particle interactions, and dewatering behavior of kaolinite dispersions”, *J. Colloid Interface Sci.*, **261**(2), 349-359. [https://doi.org/10.1016/S0021-9797\(03\)00113-9](https://doi.org/10.1016/S0021-9797(03)00113-9).
- Nabzar, L., Pefferkorn, E. and Varoqui, R. (1984), “Polyacrylamide-sodium kaolinite interactions: Flocculation behavior of polymer clay suspensions”, *J. Colloid Interface Sci.*, **102**(2), 380-388. [https://doi.org/10.1016/0021-9797\(84\)90240-6](https://doi.org/10.1016/0021-9797(84)90240-6).
- Nasser, M.S. and James, A.E. (2006), “Settling and sediment bed behaviour of kaolinite in aqueous media”, *Sep. Purif. Technol.*, **51**(1), 10-17. <https://doi.org/10.1016/j.seppur.2005.12.017>.
- Nugent, R.A., Zhang, G. and Gambrell, R.P. (2009), “Effect of exopolymers on the liquid limit of clays and its engineering implications”, *Transport. Res. Record*, **2101**(1), 34-43. <https://doi.org/10.3141/2101-05>.
- O’Brien, N.R. (1971), “Fabric of kaolinite and illite floccules”, *Clay. Clay Miner.*, **19**(6), 353-359. <https://doi.org/10.1346/CCMN.1971.0190603>.
- Palomino, A.M. and Santamarina, J.C. (2005), “Fabric map for kaolinite: Effects of ph and ionic concentration on behavior”, *Clay. Clay Miner.*, **53**(3), 211-223. <https://doi.org/10.1346/ccmn.2005.0530302>.
- Priya, K.L., Jegathambal, P. and James, E.J. (2015), “On the factors affecting the settling velocity of fine suspended sediments in a shallow estuary”, *J. Oceanogr.*, **71**(2), 163-175. <https://doi.org/10.1007/s10872-014-0269-x>.
- Revelo, C.F. and Colorado, H.A. (2018), “3d printing of kaolinite clay ceramics using the direct ink writing (diw) technique”, *Ceramics Int.*, **44**(5), 5673-5682. <https://doi.org/10.1016/j.ceramint.2017.12.219>.
- Ruhsing Pan, J., Huang, C., Chen, S. and Chung, Y.-C. (1999), “Evaluation of a modified chitosan biopolymer for coagulation of colloidal particles”, *Colloid. Surface. A: Physicochem. Eng. Aspects*, **147**(3), 359-364. [http://doi.org/10.1016/S0927-7757\(98\)00588-3](http://doi.org/10.1016/S0927-7757(98)00588-3).
- Santamarina, J.C., Klein, K.A., Wang, Y.H. and Prencke, E. (2002), “Specific surface: Determination and relevance”, *Can. Geotech. J.*, **39**(1), 233-241. <https://doi.org/10.1139/t01-077>.
- Seo, S., Lee, M., Im, J., Kwon, Y.M., Chung, M.K., Cho, G.C. and Chang, I. (2021), “Site application of biopolymer-based soil treatment (bpst) for slope surface protection: In-situ wet-spraying method and strengthening effect verification”, *Constr. Build. Mater.*, **307**, 124983. <https://doi.org/10.1016/j.conbuildmat.2021.124983>.
- Seybold, C. (1994), “Polyacrylamide review: Soil conditioning and environmental fate”, *Commun. Soil Sci. Plant Anal.*, **25**(11-12), 2171-2185.
- Shaikh, S.M.R., Nasser, M.S., Hussein, I., Benamor, A., Onaizi, S.A. and Qiblawey, H. (2017), “Influence of polyelectrolytes and other polymer complexes on the flocculation and rheological behaviors of clay minerals: A comprehensive review”, *Separat. Purification Technol.*, **187**, 137-161. <https://doi.org/10.1016/j.seppur.2017.06.050>.
- Sridharan, A. and Prakash, K. (1999), “Influence of clay mineralogy and pore-medium chemistry on clay sediment formation”, *Can. Geotech. J.*, **36**(5), 961-966. <https://doi.org/10.1139/t99-045>.
- Stokes, G.G. (1851), “On the effect of the internal friction of fluids on the motion of pendulums”, *Transactions of the Cambridge Philosophical Society*.
- Sujatha, E.R., Atchaya, S., Sivasaran, A. and Keerdthe, R.S. (2020), “Enhancing the geotechnical properties of soil using xanthan gum—an eco-friendly alternative to traditional stabilizers”, *Bulletin of Engineering Geology and the Environment*. <https://doi.org/10.1007/s10064-020-02010-7>.
- Tan, X., Hu, L., Reed, A.H., Furukawa, Y. and Zhang, G. (2014), “Flocculation and particle size analysis of expansive clay sediments affected by biological, chemical, and hydrodynamic factors”, *Ocean Dynam.*, **64**(1), 143-157. <https://doi.org/10.1007/s10236-013-0664-7>.
- Theng, B.K.G. (2012), *Formation and properties of clay-polymer complexes*, Elsevier
- Theodoro, J.D.P., Lenz, G.F., Zara, R.F. and Bergamasco, R. (2013), “Coagulants and natural polymers: Perspectives for the treatment of water”, *Plast. Polymer Technol.*, **2**(3), 55-62.
- Tombácz, E. and Szekeres, M. (2006), “Surface charge heterogeneity of kaolinite in aqueous suspension in comparison with montmorillonite”, *Appl. Clay Sci.*, **34**(1), 105-124. <https://doi.org/10.1016/j.clay.2006.05.009>.
- Toorman, E.A. (1996), “Sedimentation and self-weight consolidation: General unifying theory”, *Géotechnique*, **46**(1), 103-113. <https://doi.org/10.1680/geot.1996.46.1.103>.
- van Oss, C.J., Giese, R.F. and Costanzo, P.M. (1990), “Dlvo and non-dlvo interactions in hectorite”, *Clay. Clay Miner.*, **38**(2), 151-159. <https://doi.org/10.1346/CCMN.1990.0380206>.
- Verwey, E.J.W. (1947), “Theory of the stability of lyophobic colloids”, *J. Phys. Colloid Chem.*, **51**(3), 631-636. <https://doi.org/10.1021/j150453a001>.
- Walter, R.H. and Jacon, S.A. (1994), “Molecular weight approximations of ionic polysaccharides by ph determinations”, *Food Hydrocolloids*, **8**(5), 469-480. [https://doi.org/10.1016/S0268-005X\(09\)80089-1](https://doi.org/10.1016/S0268-005X(09)80089-1).
- Wang, Y.H. and Siu, W.K. (2006), “Structure characteristics and mechanical properties of kaolinite soils. I. Surface charges and structural characterizations”, *Can. Geotech. J.*, **43**(6), 587-600. <https://doi.org/10.1139/t06-026>.
- Watabe, Y. and Saitoh, K. (2015), “Importance of sedimentation process for formation of microfabric in clay deposit”, *Soils Found.*, **55**(2), 276-283. <https://doi.org/10.1016/j.sandf.2015.02.004>.
- Whitcomb, P.J. and Macosko, C.W. (1978), “Rheology of xanthan gum”, *J. Rheology*, **22**(5), 493-505. <https://doi.org/10.1122/1.549485>.
- White, M. (1975), *Settling of activated sludge*, Water Research Centre, England.
- White, M. (1976), “Design and control of secondary settlement tanks”, *Water Pollution Control*, **75**(4), 459.
- Winterwerp, J.C. (1998), “A simple model for turbulence induced

- flocculation of cohesive sediment”, *J. Hydraulic Res.*, **36**(3), 309-326. <https://doi.org/10.1080/00221689809498621>.
- Zbik, M.S., Smart, R.S.C. and Morris, G.E. (2008), “Kaolinite flocculation structure”, *J. Colloid Interface Sci.*, **328**(1), 73-80. <https://doi.org/10.1016/j.jcis.2008.08.063>.
- Zhou, Y., Gan, Y., Wanless, E.J., Jameson, G.J. and Franks, G.V. (2008), “Interaction forces between silica surfaces in aqueous solutions of cationic polymeric flocculants: Effect of polymer charge”, *Langmuir*, **24**(19), 10920-10928. <https://doi.org/10.1021/la801109n>.
- Zhu, P., Wang, L.Y., Hong, D., Qian, G.R. and Zhou, M. (2012), “A study of making synthetic oxy-fluoride construction material using waste serpentine and kaolin mining tailings”, *Int. J. Mineral Process.*, **104-105**, 31-36. <https://doi.org/10.1016/j.minpro.2011.12.003>.